

INTERACTION OF CARBON DIOXIDE CORROSION INHIBITORS WITH CORROSION PRODUCTS DEPOSIT

Martin Foss[#], Egil Gulbrandsen^{*#}, Johan Sjöblom[#]

*Institute for Energy Technology
Materials and Corrosion Technology Department
NO-2027 Kjeller, Norway

[#] Department of Chemical Engineering
Norwegian University of Science and Technology
NO-7051 Trondheim, Norway

ABSTRACT

The efficiency of corrosion inhibitors may be reduced in the presence of corrosion product films. In the present paper the relation between surface wettability, corrosion rate and inhibitor performance was investigated on carbon steel specimens with partly protective ferrous carbonate (FeCO_3) films in brine/oil mixtures. Two inhibitor base chemicals and a generic model compound were tested. The corrosion and inhibition tests were performed at 60 °C in 3% NaCl brine under 1 bar CO_2 . Wettability was studied by contact angle measurements on steel coupons with iron carbonate films. In absence of oil, the inhibitors had no significant effect on the corrosion rate. The presence of oil significantly enhanced the performance of some of the tested inhibitors. The addition of the inhibitors leads to a significant change in wettability of FeCO_3 for an originally oil-wet surface. For an initially water-wet surface, the FeCO_3 remained hydrophilic when inhibitors were added. It was concluded that the main effect of oil is to modify the structure of the inhibitor film.

Keywords: Oleic imidazoline, CTAB, phosphate ester, LPR, CO_2 corrosion, surface structure, iron carbonate, FeCO_3 .

Copyright

Government work published by NACE International with permission of the author(s). The material presented and the views expressed in this paper are solely those of the author(s) and are not necessarily endorsed by the Association. Printed in the U.S.A.

INTRODUCTION

Carbon steel pipelines are commonly employed in the transport of oil and gas. Carbon steel piping and process equipment are subject to corrosion caused by the presence of water and acidic gases such as carbon dioxide (CO₂), hydrogen sulfide (H₂S) and/or acetic acid (CH₃COOH). Several possible mitigation methods have been developed to reduce the corrosion rate in such pipelines to acceptable levels. The use of corrosion inhibitors and the manipulation of surface deposits are two possible ways of lowering the corrosion rate.^{1,2}

Corrosion inhibitors are widely used in the oil and gas industry to protect pipelines where the surface of the steel is in direct contact with an aqueous phase. CO₂ corrosion inhibitors typically consist of amphiphilic, surface-active molecules with hydrocarbon chains in the range C12-C18. Amphiphilic molecules have a strong tendency for self-assembly, driven by the hydrophobic effect.^{2,3} The self assembled hydrocarbon chains form structures with hydrocarbon phase properties that may change electrochemical reaction rates, influence the mass transfer of reactants or reaction products, or simply block parts of the surface, and thus reduce the active area.^{2,3} Several papers have been published regarding adsorption and inhibition by long chained hydrocarbons.^{2, 4-7} The exact mechanisms of action for the inhibitors are, however, not fully understood. Some data on the kinetics of corrosion inhibition has been published recently. Bilkova and Gulbrandsen found that the CO₂ corrosion inhibition was composed of two processes: first a rapid process (order of minutes) connected to hydrophobically driven adsorption of the inhibitor, leading to inhibition of the anodic part reaction, and a second slower process (order of hours) leading to a reduction in the corrosion rate through inhibition of the cathodic part reaction(s).⁸

Previous inhibitor testing work has demonstrated that the performance of CO₂ corrosion inhibitors in many cases was reduced when the steel was corroded before inhibition.⁹ Based on these results ferrous carbonate (FeCO₃) corrosion product deposits are expected to have an impact on the inhibitor performance. FeCO₃ deposits typically forms in systems containing CO₂ at elevated temperature and may have a positive (lower rate) effect on the corrosion rate.¹ The scaling tendency model^{10,11} gives a description of ferrous carbonate film growth and protectiveness that is consistent with most of the experimental findings.^{10,12,13} Limited data has yet been published on the interaction between this partly protective corrosion deposit and corrosion inhibitors.⁴ The corrosion deposit may reduce access of the inhibitor to the steel surface and inhibitor performance might differ significantly from what is seen on bare carbon steel surfaces.

Surfactants, such as corrosion inhibitors, might change the wetting behavior of iron and iron carbonate surfaces due to the formation of surface structures with hydrocarbon properties. The creation of a hydrophobic surface on the FeCO₃ may attract oil to the surface of the steel and reduce the corrosion rate. Some data on reservoir carbonates wetting have been published¹⁴⁻¹⁶, but to date no data has been published on the wetting behavior of iron carbonate in oxygen free environment. The influence of organic surfactants on wetting has been investigated for reservoir materials but to our knowledge no publications has been discussing the impact on corrosion.^{17,18}

The present work presents data on the performance of corrosion inhibitors on carbon steel with partly protective FeCO₃ deposits in the presence of oil. Alterations in wettability were also investigated by contact angle measurements. The main objective for the work was to obtain better understanding of how inhibitors interact with an iron carbonate covered steel surface in the presence of oil. As a starting point for our investigations, we used two CO₂ corrosion inhibitors base chemicals (a phosphate ester (PE) and an oleic imidazoline

salt) and one widely studied surfactant (cetyltrimethylammonium bromide (CTAB)) to study the interaction of surfactants and corroding steel.¹⁹ The choices of inhibitors were based on applicability to real systems and previous knowledge of the inhibitors (Table 1).

CTAB is a preferentially water-soluble quaternary ammonium compound with an aliphatic C16 chain that has been thoroughly studied as a surfactant¹⁹ as well as a corrosion inhibitor.^{8, 20-23} Recent research has shown that the CTAB molecules adsorbed on hydrophilic silica and mica forms discrete structures, i.e. admicelles.¹⁹ The surface coverage was therefore poor. Similar conclusion was reached in quartz crystal microbalance studies of CTAB adsorption onto iron and gold.^{22,23}

The oleic imidazoline salt (OI) contains an imidazoline group and a C17 hydrocarbon chain with a double bond; it is a reaction product of diethylenetriamine and a fatty acid.²⁴ Oleic imidazoline salt has been reported to partition preferentially to water. The adsorption of oleic imidazoline salt onto iron surface was found to be a fast process. Studies of oleic imidazoline by atomistic simulation methods suggest that a self-assembled monolayer forms.² Moon et al. found that the maximum of the inhibition efficiency was reached at about the same concentration as the minimum of the oil-water interface tension was reached⁷.

The detailed structure of the present phosphate ester is unknown. However, the general structure (Table 1) is a phosphate group connected to one or more hydrocarbon chains. Several authors have studied the corrosion inhibiting properties of phosphate esters.²⁵⁻²⁷ They are very effective, especially at moderate temperatures or in the presence of trace amounts of oxygen.²⁶⁻²⁸

Wettability has been widely studied on dielectric materials such as calcite (CaCO_3) and some noble metals.^{14, 18, 29, 30} Contact angle measurements have been used to determine the effect of liquids containing surface-active molecules, such as crude oil.^{14, 31, 32} In surface chemistry the term wetting refers to the extent of contact between a liquid and a solid surface. The wetting properties of a surface/liquid system are determined by the balance of forces at the line of contact between the liquid and the solid.³³ The wetting of an iron carbonate surface in an oil/water system is thus a function of the interfacial tension forces between oil and water (γ_{ow}), water and iron carbonate (γ_{sw}) and oil and iron carbonate (γ_{so}).³³ The contact angle and the surface energies of the materials involved are related by the equation (1):

$$\gamma_{sw} = \gamma_{so} + \gamma_{ow} \cos \theta \quad (1)$$

A sketch showing the direction of the forces in Equation 1 is seen in Figure 1. The reported contact angles were measured in the aqueous phase. A contact angle in the aqueous phase of 90° or greater generally characterizes a surface as hydrophobic, while an angle of less than 90° means that the surface is hydrophilic.

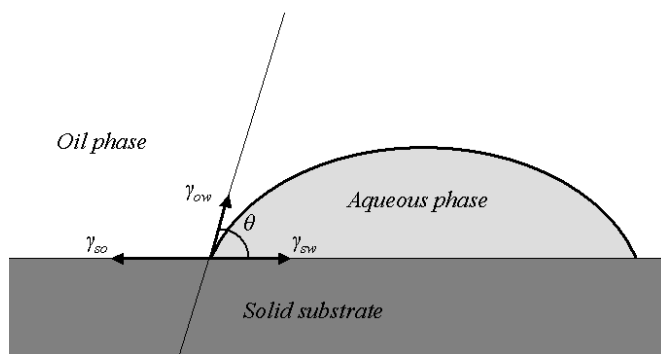


Figure 1. Sketch showing the direction of the forces acting on the line of contact between the liquids and the solid and the contact angle (θ) of the droplet.

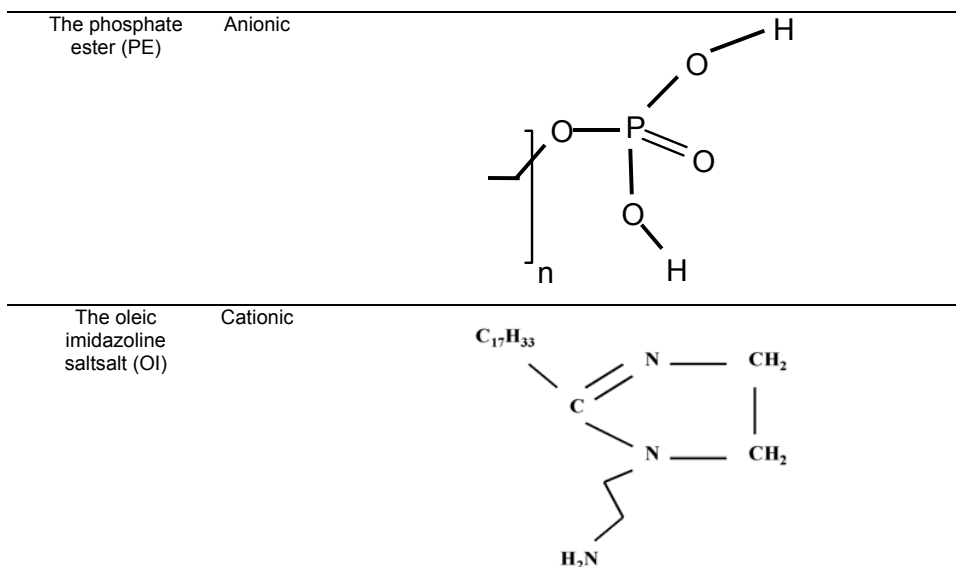
EXPERIMENTAL

Chemicals and materials

A refined, low aromatic oil product was used as model oil in the tests. It has a density of 0.788 kg/L and boiling point range 193-245 °C, corresponding to kerosene.³⁴ The Cetyltrimethylammonium Bromide (CTAB) was supplied as a powder (Aldrich), the oleic imidazoline salt was supplied as technical grade (67.5 Wt-% in a solvent), formed by reaction of diethylenetriamine and tall-oil. The phosphate ester was also supplied as a technical grade product; details of its composition are not known. The reported concentrations are referred to the supplied product. An outline of the inhibitor structures is given in Table 1. The test brine consisted of distilled water with 3 Wt% technical grade NaCl added. CO₂ gas was supplied as a 4.0 grade gas with a maximum O₂ content of 10 ppm (by volume). The critical micelle concentration (CMC) of CTAB is 7 ppm in brine with 3 Wt% NaCl.²² The CMC of the other products could not be determined, since no clear break-points were found in the surface tension versus concentration curves. Water to oil partitioning has been investigated in-house.³⁵ Preferential partitioning to water was found for all three inhibitors.

TABLE 1. INHIBITOR COMPOUNDS USED IN THE EXPERIMENTS.

Inhibitor compound	Type	Structure
Cetyltrimethylammonium Bromide (CTAB)	Cationic	$\text{CH}_3(\text{CH}_2)_{14}\text{CH}_2-\overset{\text{CH}_3}{\underset{\text{CH}_3}{\overset{+}{\text{N}}}}-\text{CH}_3 \quad \text{Br}^-$



The test specimens used in both the contact angle measurements and the corrosion inhibition experiments were machined from API X-65 ferritic-pearlitic low carbon pipeline steel (Element analysis (wt%): C, 0.08; Mn, 1.54; Ni, 0.03; Si, 0.25; Cr, 0.04; P, 0.019; S, 0.001; V, 0.045; Mo, 0.01; Al, 0.038; Nb, 0.04; Sn, 0.001).

Contact angle

The contact angles (CA) were measured with a commercially available goniometer instrument, using a liquid measuring chamber. Continuous gas purging of the measurement chamber was done to avoid oxygen contamination in the tests. Two different types of contact angle measurements were done:

1. Water droplet on iron carbonate covered steel immersed in oil (denoted water-in-oil experiments).
2. Oil droplet on an inverted iron carbonate covered steel immersed in the aqueous brine (denoted oil-in-water experiments).

The experiments were conducted at different inhibitor concentrations. The fluids and corrosion coupons used in the experiments were prepared in a separate 3-liters cell containing 2400 ml brine and 600 ml oil to ensure oil saturation of the brine, and inhibitor partitioning similar to the corrosion experiments. Formation of FeCO_3 was achieved by corroding several test specimens in a glass cell for more than 200 hours. The temperature during the iron carbonate film formation was $75\text{ }^\circ\text{C}$. The electrolyte was bubbled with CO_2 at ambient pressure at least 3 hours prior to immersion of the coupons to saturate with CO_2 and deoxygenate the solution. The CO_2 pressure was about 0.6 bar (water vapor pressure 0.4 bar). Flat steel coupons (25 mm by 25 mm, 3 mm thick) were used in the tests. They were prepared by grinding with 1000 mesh SiC paper followed by cleaning with technical acetone in an ultrasonic bath. Shortly before immersion in the test solution the samples were cleaned with isopropanol. All samples were mounted on a horizontal sample holder placed in the glass cells. The first inhibitor dose was added 1 hour after the oil, and the concentration was increased in steps with intervals of 1 hour. One sample was removed

before each new inhibitor concentration increase. The exposure time to the tested concentration was therefore 1 hour. The samples were rapidly lifted through the oil layer, and dried by blowing pressurized CO₂ onto the surface of the steel to rid the steel surface of the liquid film covering the surface. The dry sample was then immersed in the contact angle cell, which was filled with either oil or brine sampled from the precorrosion cell. The oil-in-water experiments were done with an inverted surface where the droplet was deposited on the surface using the droplet flotation. SEM pictures were taken of a cross section of several of the specimens after termination of the tests to ensure that the iron carbonate films were comparable for all the tests.

Corrosion experiments

Corrosion experiments were carried out on stationary cylinder (10 mm diameter, 10 mm length and 3.14 cm² exposed area) specimens in a 3-liters thermostatted glass cell at ambient pressure. The steel specimens were ground with 1000 mesh SiC paper wetted with isopropanol, cleaned with technical acetone in ultrasonic bath and flushed with ethanol. The electrolyte solution preparation was identical to that of the contact angle measurements except for the amount of oil. Only 15 ml of oil was used to saturate the aqueous phase with oil. The solution was continuously purged with CO₂ at ambient pressure throughout the experiments. The pH of the system was initially around pH 3.9. The pH increased to above 6 before initiation of the iron carbonate layer. The increased pH is caused by formation of HCO₃⁻ in the cathodic reaction. After iron carbonate formation was initiated the pH decreased to 5.7 due to the reduction in HCO₃⁻ concentration caused by the precipitation of iron carbonate. The corrosion experiment can be divided into two stages.

1. Formation of the FeCO₃ layer: Formation of FeCO₃ was achieved by the same technique as for the contact angle measurements. The total corroding surface area in the corrosion tests corresponded to approximately 20 cm²/L. Corrosion rates were measured by on one or more of the specimens. A partly protective FeCO₃ layer started to form after approximately 100h. The FeCO₃ layer formation was stopped after about 200h. The corrosion had dropped to approximately 0.5 mm/y after the FeCO₃ formation stage. After iron carbonate formation the different specimens were moved rapidly to prepared test cells containing a supersaturated Fe²⁺ brine.
2. Inhibitor testing on the FeCO₃ covered specimens: The corrosion testing was performed at 60 °C, to facilitate comparison with other results. The inhibitor was added from a 3 % NaCl stock solution.

Two types of experiments were conducted:

1. Corrosion in brine without oil added, with different concentrations of inhibitor
2. Corrosion in brine saturated with oil with different concentrations of inhibitor. The sample was also periodically immersed in the oil. 20 Wt% of model oil was added to all the test cells before the inhibitor was added. This was done to saturate the water phase with the oil components (mainly aliphatic hydrocarbons).

A three-electrode setup was used for the electrochemical measurements. An Ag/AgCl (3 M KCl) electrode and a titanium ring surrounding the working electrode were used as reference and auxiliary electrode, respectively. The Polarization Resistance technique³⁶ (LPR) was used to monitor the corrosion rate. Measurements were done at 30 min. intervals throughout the test. The potential was scanned from -5 mV to +5 mV vs. the

open-circuit potential with rate 0.1 mV/s. The polarization resistance (R_p) was corrected for uncompensated electrolyte resistance measured by electrochemical impedance spectroscopy. The corrosion current density (I_{cor}) was calculated from R_p using equation (2):

$$I_{cor} = B/(A R_p) \quad (2)$$

where A is the exposed surface area of the test electrode and B is a constant. In the case of simple activation controlled reactions the value of the B can be determined from the Tafel slopes of the part reactions²⁷ by equation (4).

$$B = \frac{b_a b_c}{2.303(b_a + b_c)} \quad (3)$$

where b_a and b_c are the Tafel slopes of the anodic and cathodic polarization curves, respectively. Empirical B-values are commonly applied in the CO₂ corrosion field due to the complexity of the polarization curves.³⁷⁻³⁹ This complexity is caused by the different cathodic reactions taking place in CO₂ corrosion.³⁹ Anodic Tafel slopes in the range 40-60 mV are reported³⁷. B-values of 20 ± 5 mV are typically obtained for uninhibited CO₂ corrosion by calibration to mass loss.³⁸ This is consistent with b_a -values in the range 40-60 mV and b_c being infinite. In most cases of inhibited CO₂ corrosion the cathodic polarization curves normally show Tafel behavior (b_c about 120 mV), but the anodic polarization curves often deviate from Tafel behavior at higher polarization. A more detail discussion on the determination of the value of the B constant can be found in ref. [39]. An empirical value of 20 mV³⁸⁻³⁹ was used for B in all the reported data. In this way the reported results are also proportional to $1/R_p$ and thus reflect the changes in the measured parameter. The corrosion rate is reported in mm/y, and is obtained from the corrosion current using Faraday's law calculation according to the anodic dissolution reaction $Fe = Fe^{2+} + 2 e^-$, and using 7.9 g/cm³ as the density of the steel.

RESULTS

Contact angle – water-in-oil

A plot of contact angles versus inhibitor concentration for tests containing OI, PE and CTAB are plotted in Figure 2. The contact angle of the inhibitor-free water-phase was 40° in this system. Additions of OI or PE lead to a transition from a hydrophilic to a hydrophobic surface. The tendency was seen for all concentrations of OI and PE. When CTAB was used complete water wetting (CA < 5°) was found for all inhibitor concentrations. The exact contact angle was not measurable due to the very low contact angles. The contact angle for OI increased to 140° for concentrations above 20 ppm inhibitor, at which point the curve seemed to reach a stable value. A contact angle of more than 155° was found for PE at concentrations of 20 ppm and above. No time trend is shown due to the lack of any significant change in contact angle with time.

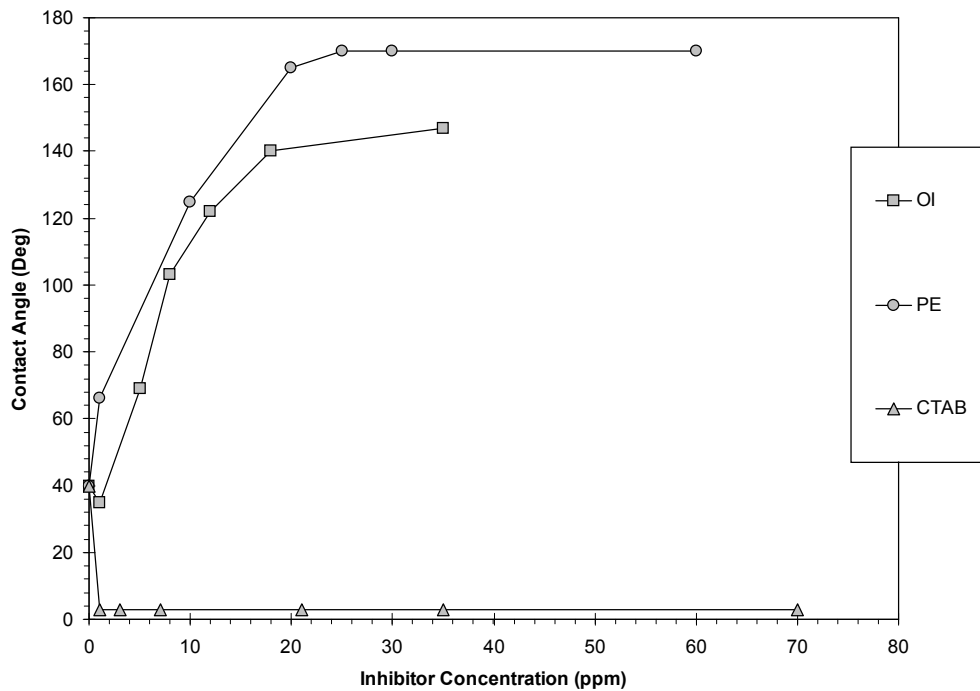


Figure 2. Contact angle for water-in-oil experiments for OI, PE and CTAB on iron carbonate. Experimental conditions: 1 bar CO₂, 3% NaCl, and ambient temperature.

An illustration of the large difference in CA obtained in the PE and the CTAB tests at high concentrations is seen in Figure 3. When the calculated contact angles exceeded 160° or more, the droplet rolled off the surface if a tilt was introduced. This indicates a super-hydrophobic behavior where the contact angle approaches 180°, which could not be detected by the instrument software.

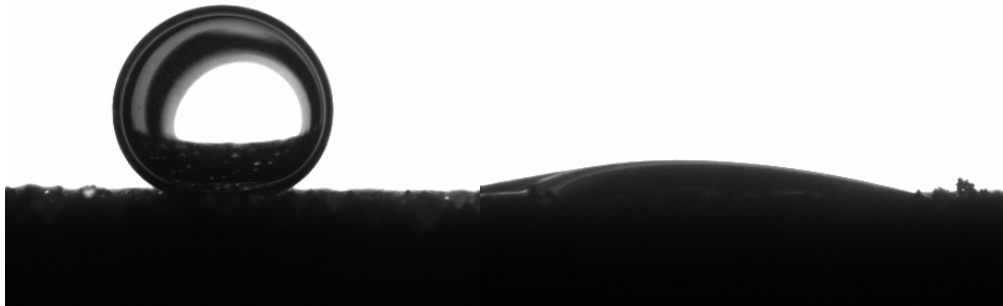


Figure 3. Photos of the water droplet in a test with a concentration of 60 ppm PE (left) and a test with a concentration of 21 ppm CTAB (right). Both pictures were captured approximately 50 seconds after deposition of the droplet.

Contact angle – oil-in-water

Figure 4 shows contact angles measured in the water-phase for tests where the iron carbonate surface was exposed to the inhibited brine. The contact angle in the uninhibited

water-phase was approximately 17°. Addition of inhibitor caused some scatter in the recorded contact angles for all three inhibitors, but the surface remained hydrophilic at all concentrations.

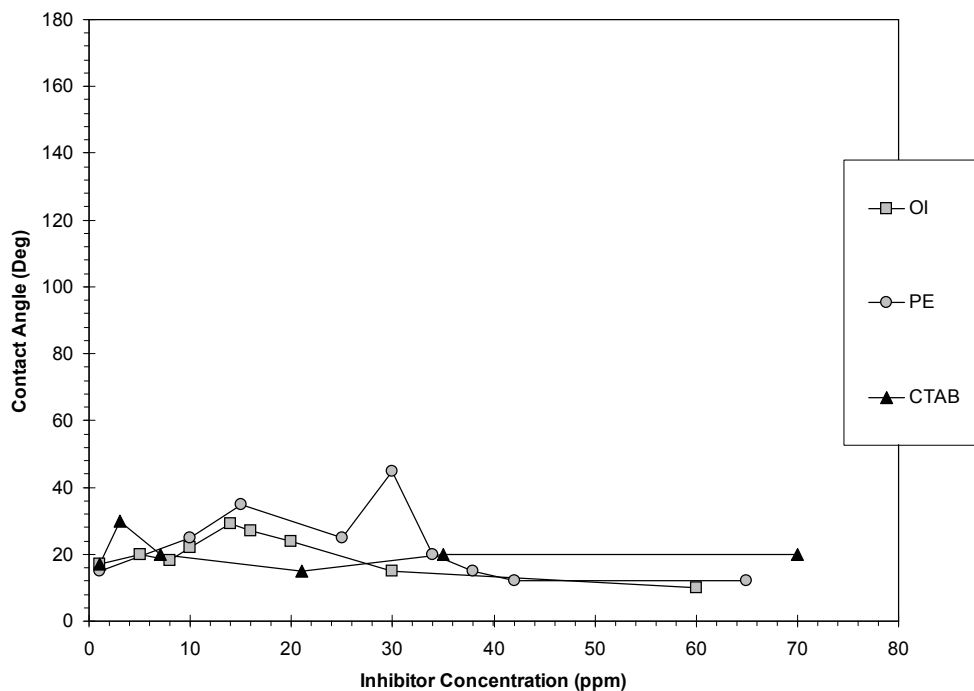


Figure 4. Contact angle for oil-in-water experiments containing the oleic imidazoline salt on iron carbonate. Experimental conditions: 1 bar CO₂, 3% NaCl, ambient temperature.

The small change in CA obtained at intermediate concentrations of PE is seen in Figure 5.

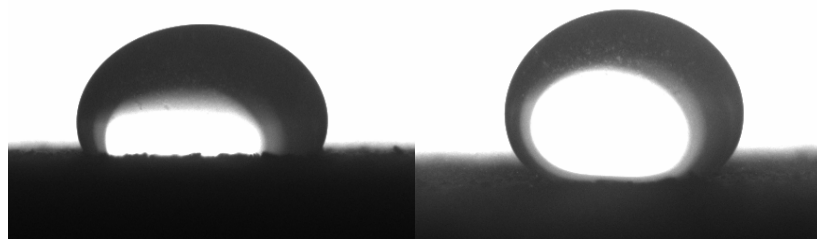


Figure 5. Photos of the oil droplet in the test containing PE at two different concentrations of the inhibitor. At 30 ppm (left) and at 42 ppm (right). Both pictures were captured approximately 50 seconds after deposition of the droplet, and are rotated 180 °C.

Corrosion inhibition experiments

CTAB: Introductory corrosion test in pure aqueous phase showed that this compound was not able to inhibit CO₂ corrosion on unprotected carbon steel. The same

result was expected for iron carbonate covered specimens and tests without oil are therefore not included.

Figure 6 shows the results for a test with CTAB in presence of a small amount of oil. A partly protective film of FeCO_3 was formed after approximately 190 h of the test, lowering the corrosion rate to below 0.5 mm/y. The temperature was thereafter lowered from 80 °C to 60 °C before inhibitor and oil was added. The change in temperature did not have a significant impact on the corrosion rate in this test. After 198 h of testing 0.05 vol-% of oil was added to the test cell in order to saturate the brine with oil. The addition of oil did not affect the corrosion rate in any significant way. No reduction in the corrosion rate was observed for concentrations lower than 100 ppm. When the inhibitor concentration was increased to 200 ppm towards the end of the test, the corrosion rate started decreasing after an initial increase following the inhibitor addition. Addition of 0.5 % oil did not have any further effect on this behavior. The rate was ca. 0.2 mm/y at the end of the test, with a slowly decreasing trend. The corrosion potential increased from -620 mV to -590 mV during the course of the test.

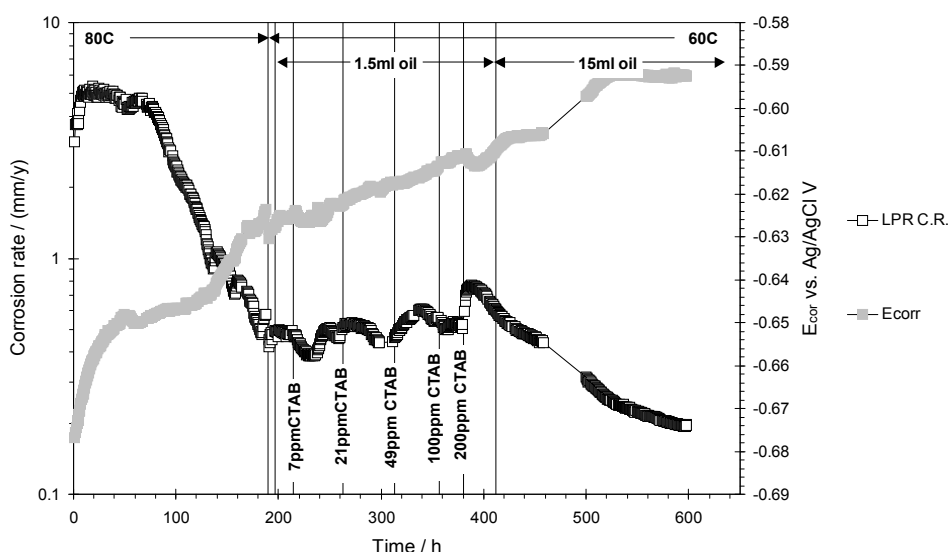


Figure 6. LPR corrosion rate and E_{corr} vs. time. FeCO_3 film formation for 190 h at 80 °C. Experimental conditions: CTAB as inhibitor, 15 ml oil, 60 °C (0.8 bar CO_2).

The oleic imidazoline salt: Figure 7 shows corrosion rate versus time for a test where only OI was added. An iron carbonate layer was grown at 80 °C for more than 300 h until a stable corrosion rate had been reached. The corrosion rate was then 0.2 mm/y. Following the temperature change from 80 °C to 60 °C an increase in the corrosion rate was seen. The corrosion rate increased from 0.2 mm/y to 1 mm/y, before it started decreasing again. This might be caused by cracking of the FeCO_3 layer. A sudden drop in corrosion potential, from -580 mV to -620 mV, was also seen after the temperature change. The potential increased towards the value it had before the temperature change once the sudden drop had stabilized. The addition of 0.1 and 0.5 ppm OI did apparently not have any effect on this behavior. After 300 h the corrosion rate had dropped to below 0.3 mm/y and a more stable corrosion rate was observed. Consecutive additions of OI up to a total concentration of 20 ppm did not show any significant effect of the inhibitor. The corrosion rate had decreased to between 0.1 mm/y and 0.2 mm/y after more than 800 h of testing. The corrosion rate was still decreasing at this point.

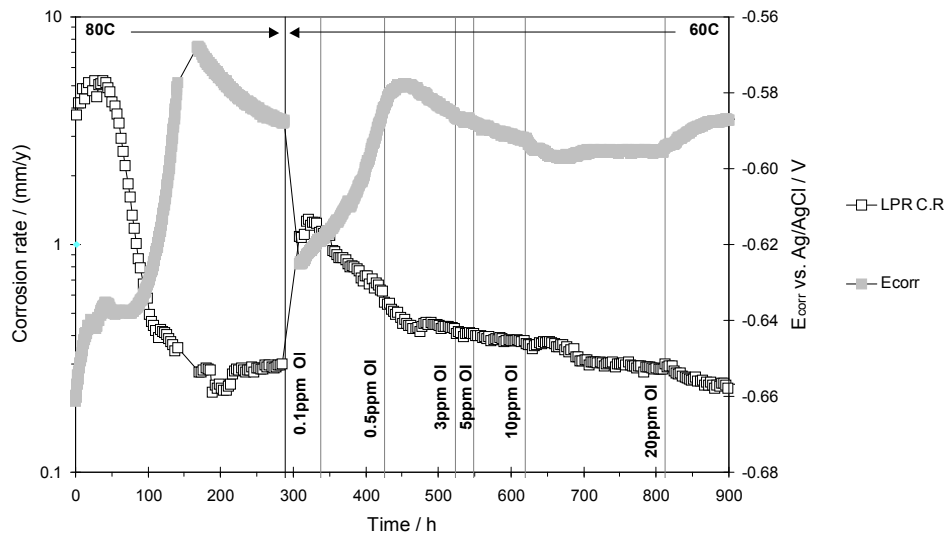


Figure 7. LPR corrosion rate and E_{corr} vs. time. $FeCO_3$ film formation for 290 h at 80 °C. Experimental conditions: OI as inhibitor, no oil, 60 °C (0.8 bar CO_2).

Figure 8 shows corrosion rate versus time for a test with OI where the sample was periodically exposed to oil. $FeCO_3$ was formed for 300 h at 80 °C. The corrosion rate stabilized around 0.45 mm/y before the temperature was changed to 60 °C. No significant change in corrosion rate was seen after the change in temperature. Addition of 20 Wt% oil to the test cell did not affect the corrosion rate. Addition of oleic imidazoline salt up to a concentration of 10 ppm lead to a slight decrease in the corrosion rate. Periodic exposure to oil did not have any significant impact on the corrosion rate below this concentration. When the concentration was increased to 20 ppm a significant drop in the corrosion rate could be seen; the rate had dropped to 0.03 mm/y after 400 h. A transient, but significant, effect of the oil exposure was seen at this concentration. The decrease in corrosion rate was accompanied by a large increase in the corrosion potential.

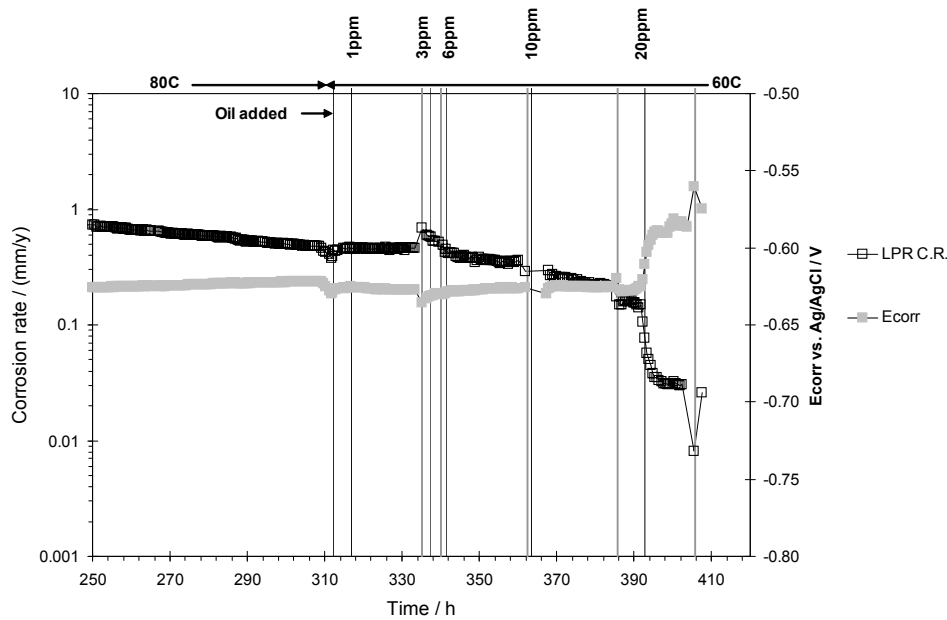


Figure 8. LPR corrosion rate and corrosion potential as a function of time. FeCO_3 was formed for 300 h at 80 °C. Oil exposures are indicated by grey lines. Experimental conditions: OI as inhibitor, 20 Wt% oil, 60 °C (0.8 bar CO_2).

The phosphate ester compound: Figure 9 shows the corrosion rate versus time for a test with PE without oil. The corrosion rate stabilized below 0.2 mm/y after the carbonate layer build-up, but increased to 1mm/y after the change from 80 °C to 60 °C. This behavior is similar to what was seen in Figure 7. After this increase in corrosion rate a steady decrease towards the corrosion rate after FeCO_3 growth was seen. This decrease seemed to be affected by the stepwise addition of PE. The corrosion potential also showed a stepwise change depending on the PE addition, increasing from -640 mV at the beginning of the test to -590 mV at the end. After more than 600 h the corrosion rate was almost stable and had dropped to below 0.2 mm/y. No further effect on the corrosion rate and potential was found for concentrations above 70 ppm PE.

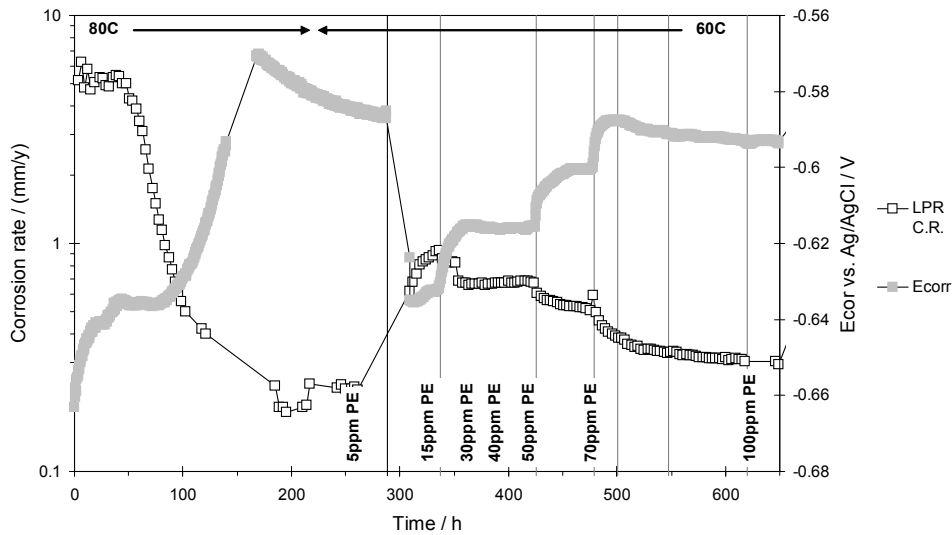


Figure 9. LPR corrosion rate and E_{cor} vs. time. FeCO_3 film formation for 280 h at 80 °C. Experimental conditions: PE as inhibitor, no oil, 60 °C (0.8 bar CO_2).

Figure 10 shows corrosion rate versus time for a test with PE where the sample was periodically exposed to oil. FeCO_3 was formed for 300 h at 80 °C. The corrosion rate stabilized around 0.35 mm/y before the temperature was changed to 60 °C. No significant change in corrosion rate was seen after the change in temperature. Addition of 20 Wt% oil to the test cell did not affect the corrosion rate. Increasing the concentration of PE to 10 ppm and then to 20 ppm lead to a reduction in corrosion rate to 0.05 mm/y. No lasting effect of the direct exposure to the oil was seen. When the concentration was increased to 35 ppm a significant drop in the corrosion rate was seen; the rate had dropped to 0.005 mm/y after 380 h. Further increasing the concentration beyond 35 ppm did not have any significant effect on the corrosion rate. The decrease in corrosion rate was accompanied by a large increase in the corrosion potential which increased to -550 mV by the end of the test.

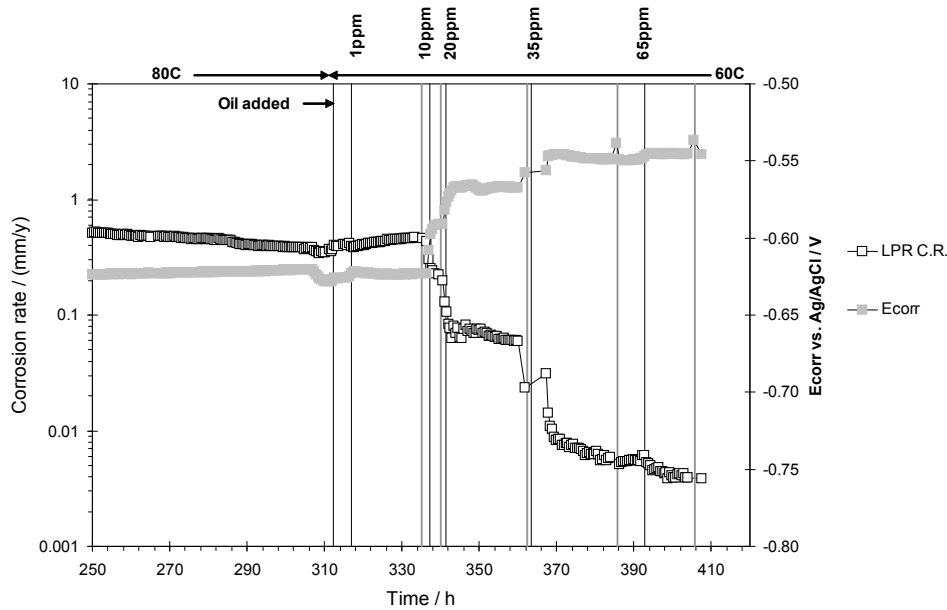


Figure 10. LPR corrosion rate and E_{cor} vs. time. $FeCO_3$ film formation for 300 h at 80 °C. Oil exposures are indicated by grey lines. Experimental conditions: PE as inhibitor, 20 Wt% oil, 60 °C (0.8 bar CO_2).

Bode plots: Figure 11 and 12 shows Bode plots for the impedance measured in the tests with OI and PE, respectively. The uncompensated solution resistance (R_u) and the combined solution and polarization resistance ($R_{ct}+R_u$) can be found at the high and low frequency plateaus of the modulus curves, respectively. R_u may comprise the resistances of the electrolyte, the $FeCO_3$ film, and a possible oil layer at the surface or in the film. In the test with OI the polarization resistance increased from an initial 30 ohms to more than 240 ohms at the end of the experiment. A change in uncompensated solution resistance (R_u) was also seen. An increase from an initial value of 1 ohm up to 5.6 ohms at the end of the test was seen. The data plotted in Figure 12 shows that the effect of the inhibitor on the uncompensated solution resistance was on a similar level for PE. An increase from 1 ohm to more than 12 ohm resistance was observed. In the test where PE was used the polarization resistance increased from 10 ohm to more than 8000 ohms. A low frequency plateau could not be located and a definite value for R_{ct} was therefore not measured.

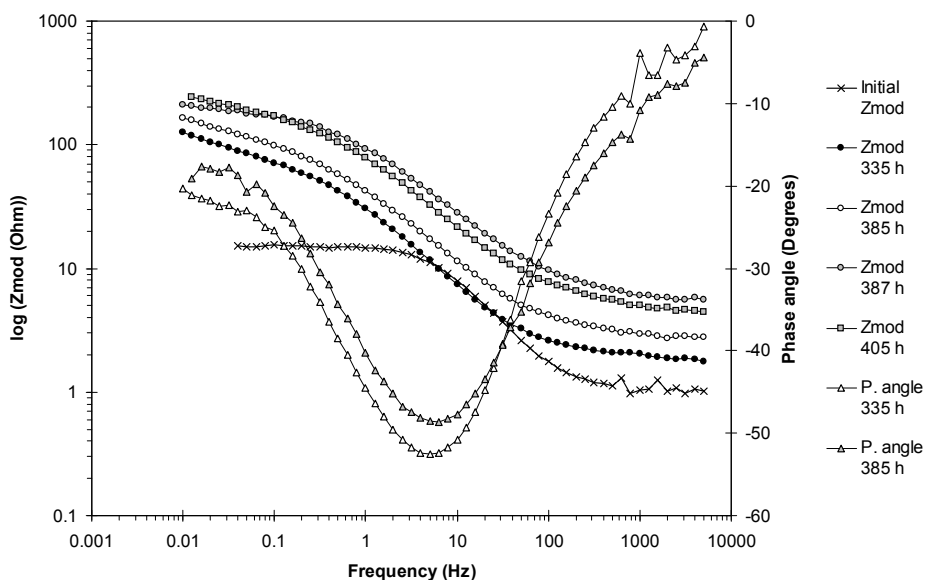


Figure 11. Bode plot showing the modulus of the impedance (Z_{mod}) and the phase angle at different stages of the experiment with OI and oil exposure. The LPR corrosion rate curve for this experiment is given in Figure 8.

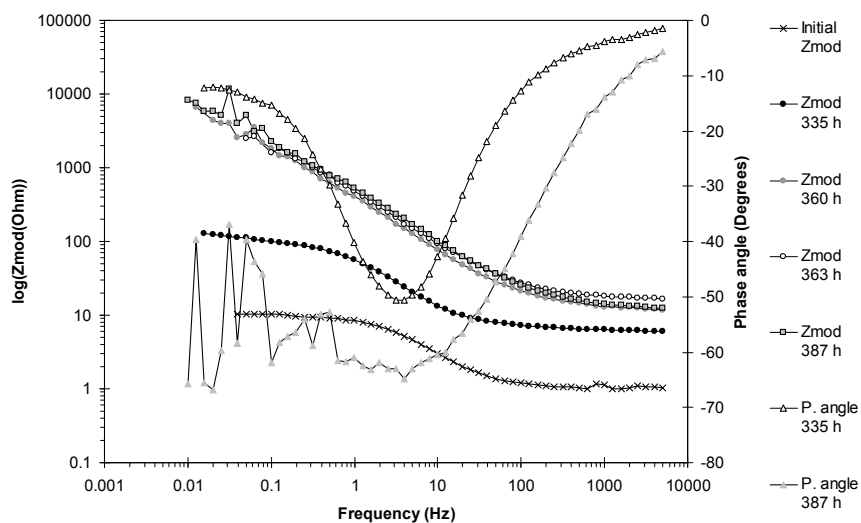


Figure 12. Bode plot showing the modulus of the impedance (Z_{mod}) and the phase angle at different stages of the experiment with PE and oil exposure. The LPR corrosion rate curve for this experiment is given in Figure 10.

DISCUSSION

The corrosion rate experiments clearly demonstrated a significant effect of oil on the performance of both the phosphate ester and the oleic imidazoline salt. The addition of oil lead to a corrosion rate one order of magnitude lower than what was found without oil for

these two inhibitors. The observed stabilization of the hydrophobic surface in the water-in-oil experiments and the improved effect of the inhibitors in the presence of oil will be the main focus of the discussion.

The focus of the contact angle measurements was to obtain results that may be relevant to a field situation. The oil-in-water experiments simulates the wetting behavior at a surface that is initially water wet, such as the bottom of a pipe with stratified flow or stagnant pools of water at low points in a pipeline. Oil dispersed in the water phase might, in stratified flow, hit the surface and interact with it and a potentially beneficial transition from a water-wet to an oil-wet surface could be achieved. The water-in-oil experiments were used to simulate the opposite situation where water droplets entrained in the oil-phase interact with an initially oil-wet surface. In this case the beneficial effect would be to avoid water droplets attaching to the steel wall and spread out, and thus wet the steel.

Figure 2 shows a significant difference between the different inhibitors. The addition of CTAB increased water wetting and concentrations as low as 1 ppm lead to a highly hydrophilic surface. CTAB is known to emulsify oil⁴⁰ and may have a detergent effect. Oil removal and emulsification by CTAB is therefore a possibility. This replacement of the oil film with a water-phase could explain the very low contact angles found for CTAB. Removal of oil film below the water droplet by solubilization of oil in the CTAB micelles might contribute to the low contact angles. The development of hydrophilic inhibitor aggregates of CTAB on the steel surface might also explain the hydrophilic behavior. For low concentrations of inhibitor the monomers are expected to adsorb individually. At higher concentrations (CMC and above) the development of a structured CTAB layer might be expected. Atkin et. al. reported hemicelles and worm-like structures of CTAB on graphite for concentrations of around CMC and above.¹⁹ The change in the wetting properties of the steel might be explained by this effect but, to our knowledge, no studies on the structure of CTAB on corroding steel has been published to date. An ordered surfactant structure of this kind is also possible for both OI and PE, but the results for the contact angle of water in oil suggest a different structure. OI and PE both increased the hydrophobicity dramatically of the oil-wet surface. In the field relevant situation this effect might lower the steel pipe wall's affinity to water and thus prevent water droplets from wetting and spreading on an already oil-wet surface. No significant effect of time was found for any of the tests.

For an initially water-wet surface the effect of added inhibitor did not have the impact it had in the system with an initially oil-wet surface, and the surface remained hydrophilic (Figure 4). This indicates that it is difficult to form an oil film on a water-wet FeCO_3 surface. The data shows that the addition of the inhibitors lead to some scattering of the contact angles at intermediate inhibitor concentrations. For CTAB the apparent peak in hydrophobic tendencies was 3 ppm inhibitor. For OI and PE the apparent peak in hydrophobic behavior lay around 14 ppm and 30 ppm respectively. The increased hydrophobic tendencies might be caused by the structure of the surface-layer of inhibitor. This behavior is not considered to be important to field conditions due to the very limited effect observed.

The corrosion tests were conducted to investigate the impact of oil on the corrosion rate in inhibited systems of iron carbonate covered steel. As mentioned the introduction of oil into the solution drastically improved the performance of OI and PE. The tests with oil and OI or PE were reduced around one order of magnitude or more in the presence of oil. It is clear that the presence of oil leads to a change in the way the inhibitor interacts with the iron carbonate covered steel surface. The reduction in corrosion rate may be caused by various mechanisms. The two most likely mechanisms are: 1) a modification of the iron carbonate layer caused by the presence of oil and 2), a modification of the inhibitor film by oil.

The first alternative assumes that the oil changes the movement of liquid at the surface of the steel by reducing diffusion and convection. This might be caused by a densification of

the iron carbonate or a possible imbibition of oil in the iron carbonate. According to the scaling tendency model reduced convection is one of the parameters leading to the development of a dense carbonate layer.¹¹ A more dense carbonate layer then reduces the access of reactants to the surface and thereby the corrosion rate. If a reduced diffusion in the carbonate layer or the imbibition of oil in the iron carbonate is the reason for the significant reduction in corrosion rates observed in Figures 8 and 10, this would be detected through the impedance measurements. A major change in the protectiveness of the FeCO₃ layer is expected to be associated with a substantial increase in the uncompensated solution resistance. As seen in Figures 11 and 12 an increase in uncompensated solution resistance is seen, but the increase is by no means large enough to account for the increase of the total resistance at low frequencies, and the magnitude of the drop in corrosion rates observed.

The impedance measurements show that the addition of inhibitor leads to a large increase in the polarization resistance of the system. The results support the idea that the oil enhanced the efficiency of the inhibitor film. This might be caused by co-adsorption of inhibitor molecules and hydrocarbons from the oil phase. The increased performance of the inhibitor through enhanced performance of the inhibitor film is thus the most probable explanation for the effect of oil.

CONCLUSION

The effect of carbon dioxide corrosion inhibitors on the wettability of iron carbonate covered carbon steel was investigated. Also investigated was the effect of oil on the performance of these inhibitors. The key findings can be summarized in five main points:

- The presence of the oleic imidazoline salt or the phosphate ester leads to the development of a highly hydrophobic steel surface for an initially oil-wet surface. The ability of an oil-wet steel surface to repel water droplets is thus greatly enhanced by these inhibitors. The PE and the OI made the initially oil-wetted FeCO₃ surface hydrophobic, and therefore improved its ability to repel impinging water droplets.
- CTAB increases the water wettability of initially oil-wet steel even at very low concentrations. This effect can be explained by a detergent effect or the formation of hydrophilic inhibitor films. CTAB improved the ability of water droplets to spread out on the oil-wetted FeCO₃ surface.
- The presence of dissolved hydrocarbons in the brine improved the inhibitor performance of both the oleic imidazoline salt and the phosphate ester significantly. The performance of the oleic imidazoline salt and the phosphate ester improved dramatically after a direct exposure of the test specimen to the oil phase.
- The results indicate that oil influence the structure of the inhibitor film to improve the protectiveness. The evidence suggests that the improved performance is caused by a co-adsorption effect rather than the formation of a microscopic and stable oil film.

ACKNOWLEDGEMENTS

The work is a part of a joint project between Institute for Energy Technology and the Norwegian University of Science and Technology, sponsored by the Research Council of Norway (Project no. 158913/I30).

REFERENCES

1. A. Dugstad, CORROSION/98, Paper no. 31, (Houston, TX: NACE International, 1998).
2. S. Ramachandran, B. Tsai, M. Blanco, H. Chen, Y. Tang and W. A. Goddard, Langmuir 12, 6419 (1996).
3. D. Fennel Evans and H. Wennerström, The colloidal domain, 2 edition (Wiley-VCH, New York, 1999).
4. I. L. Rozenfield, Corrosion Inhibitors, (McGraw-Hill, New York, 1981), p. 67.
5. P. Li, J. Y. Lin, K. L. Tan and J. Y. Lee, Electrochimica Acta 42, 4 (1997): p. 605.
6. S. Meng, E. G. Wang, S. W. Gao, Journal of Chemical Physics 119 (2003), 15.
7. T. Moon and D. Horsup, CORROSION/02, Paper no. 298, (Houston, TX: NACE International, 2002).
8. K. Bilkova, E. Gulbrandsen, M. Knag, J. Sjöblom, Kinetic study of model corrosion CO₂ inhibitors, Proceedings of the 10th European Symposium on Corrosion and Scale Inhibitors, Ann. Univ. Ferrara, N.S., Sez. V, Suppl., 2005. Ferrara, Italy, N. 12, 2005. p. 585.
9. E. Gulbrandsen, S. Nestic, A. Stangeland, T. Burchardt, B. Sundfær, S.M. Hesjevik, S. Skjerve, CORROSION/98, Paper no. 13, (Houston, TX: NACE International, 1998).
10. E.W.J. van Hunnik, et al, CORROSION/96, Paper no. 6, (Houston, TX: NACE International, 1996).
11. S. Nestic, K.-L. J. Lee, V. Ruzic, CORROSION/01, Paper no. 40, (Houston, TX: NACE International, 2001).
12. K. Chokshi, W. Sun, S. Nestic, CORROSION/05, Paper no. 285, (Houston, TX: NACE International, 2005).
13. M.L. Johnson, M.B. Tomson, CORROSION/91, Paper no. 268, (Houston, TX: NACE International, 1991).
14. D. C. Standnes and T. Austad, Journal of Petroleum Science and Engineering, 39 (2003), p 431.
15. D. C. Standnes and T. Austad, Colloids and Surfaces A - Physicochemical and Engineering Aspects, 216 (2003), Issue 1-3
16. S. Strand, E. Hognesen, T. Austad, Colloids and Surfaces A – Physicochemical and engineering Aspects, 275 (2006), 1-10.
17. C. Legens, T. Palermo, H. Toulhoat, A. Fafet, and P. Koutsoukos, Journal of Petroleum Science and Engineering, 20 (1998), p. 277
18. K. A. Rezaei Gomari and A. A. Hamouda, Journal of Petroleum Science and Engineering, 50 (2006), p. 140
19. R. Atkin, V. S. J. Craig, E. J. Wanless, S. Biggs, Advances in Colloid and Interface Science 103 (2003), p. 219.
20. G. Schmitt, B. N. Labus, H. Sun, N. Stradmann, Synergisms and Antagonisms in CO₂ Corrosion Inhibition, Proc. 8th European Symposium on Corrosion Inhibitors, Ann. Univ. Ferrara, N.S., Sez. V, Suppl. N.. 10, 1995.
21. G. Schmitt and B.N. Labus, CORROSION/94, Paper no.37, (Houston, TX: NACE International, 1994).

22. M. Knag, J. Sjöblom, G. Øye, E. Gulbrandsen, *Colloids and Surfaces A – Physicochemical and engineering Aspects* 250 (2004): p. 269.
23. M. Knag, J. Sjöblom, E. Gulbrandsen, *Journal of Dispersion Science and Technology* 26 (2005): p. 207.
24. A. J. McMahon, *Colloids and Surfaces* 59 (1991): p. 187.
25. B. Alink et. al., "Mechanisms of CO₂ Corrosion Inhibition by The phosphate ester", Supplement to *Materials Performance*, march 1999, NACE, p. 8.
26. R.L. Martin and R. Annad, *Corrosion* 37, 5 (1981): p. 297.
27. R.L. Martin, *Materials Performance* 22, 9 (1983): p. 33.
28. Y. Wu, K.E. McSperitt and G.D. Harris, *CORROSION/88*, paper no. 365, (Houston, TX: NACE International, 1988).
29. C. Drummond and J. Israelachvili, *Journal of Petroleum Science and Engineering*, 33 (2002), 243-259.
30. D. Y. Wang, H. W. Duan and H. Mohwald, *Soft Matter* 1, 6 (2005).
31. S. Hoiland, T. Barth, A. M. Blokhus and A. Skauge, *Journal of Petroleum Science and Engineering* 30, 10 (2001).
32. Horsthemke and J. J. Schroder, *Chemical Engineering and Processing*, 19 (1985), Issue 5.
33. P. Atkins, J. de Paula, "Atkins' Physical chemistry", 7th edition (Oxford University Press, 2002), p. 154.
34. www.shellchemicals.com, Data sheet: Shellsol D-70, Issued 27-may-2005
35. M. Foss – Unpublished data
36. J. R. Scully, Electrochemical tests, in: R. Baboian (Ed.), *Corrosion Tests and Standards*, Philadelphia: American Society for Testing and Materials, 1995.
37. S. Nestic, J. Postlethwaite, S. Olsen, *Corrosion* 52 (1996): p. 280.
38. W. J. Lorenz, F. Mansfeld, *Corrosion Science* 21 (1981): p. 647.
39. E. Gulbrandsen, J. Kvarekvål, H. Miland, *Corrosion* 61, 11 (2005): p. 1086.
40. G. Gutiérrez Á: Cambiella, J. M. Benito, C. Pazos and J. Coca, *Journal of Hazardous materials* 144, 3 (2007): p. 649.